

Efficiency of ZnO photocatalysts doped with La and Ag

K. I. Milenova^{1*}, K. L. Zaharieva¹, I. D. Stambolova², V. N. Blaskov², A. E. Eliyas¹

¹*Institute of Catalysis, Bulgarian Academy of Sciences, Acad. G. Bonchev St., bl. 11, 1113 Sofia, Bulgaria*

²*Institute of General and Inorganic Chemistry, Bulgarian Academy of Sciences, Acad. G. Bonchev St., Bl. 11, 1113 Sofia, Bulgaria*

Submitted on June 27, 2016; Revised on November 11, 2016

The photocatalytic efficiency of Ag and La doped ZnO materials, obtained using the impregnation followed by thermal treatment, was studied and compared in the reaction of oxidative degradation of RB5 dye as model contaminant in aqueous solutions under UV irradiation. The structure, phase composition, morphology and specific surface area of the non-doped and doped ZnO photocatalysts were investigated by Powder X-ray diffraction analysis, Scanning electron microscopy and BET method. The results indicated that the highest degree of degradation of RB5 dye (69%) after 120 minutes of illumination was achieved using La doped ZnO photocatalyst, comparing with the degree of degradation over the others samples - Ag doped ZnO (35%) and non-doped ZnO (20%). The apparent rate constants of RB5 dye degradation decrease in the following order: La-ZnO ($9.2 \times 10^{-3} \text{ min}^{-1}$) > Ag-ZnO ($3 \times 10^{-3} \text{ min}^{-1}$) > ZnO ($1.4 \times 10^{-3} \text{ min}^{-1}$) due to the interplay of La²⁺ and La³⁺ ion pair.

Keywords: ZnO, dopants, photocatalytic oxidation, Reactive Black 5.

INTRODUCTION

Developing effective and green methods for pollutants removal (among them dyes from textile industry) is important environmental hot topic of the day [1]. Heterogeneous photocatalysis using semiconductors has demonstrated its productivity in this aspect, especially in degrading persistent organics into CO₂ and H₂O or into easily biodegradable compounds [2, 3]. ZnO is among the most popular photocatalysts for dyes degradation due to its ability to absorb a wide solar spectrum [1, 4]. An effective approach for decreasing the recombination of photo-generated charge carriers and enhancing photoactivity is the modification of ZnO using doping with metals or nonmetals, metal deposition and coupling with other semiconductors [5].

The activities of Ag/ZnO samples were investigated by photodegradation of aqueous solution of Acid Blue 113, Rhodamine B, Basonyl Violet and Methylene Blue dyes under UV illumination [6-11]. Ag/ZnO photocatalysts were evaluated by the dye degradation also under direct sunlight [12-15]. Mechanism of photodegradation of Methyl Orange [16-18] and Methylene Blue dye on Ag/ZnO nanocomposites for UV and visible-light was studied [16, 17, 19]. ZnO nanosheets were hybridized with Ag₃PO₄ nanoparticles and their photocatalytic activity for the degradation of Rhodamine B dye under visible-light illumination was investigated [20]. The Fenton-like photocatalytic activity for the degradation of

Rhodamine B and Methylene Blue in the mixed dye solution using Ag/ZnO hybrid samples was studied [21]. Photodegradation of dye mixtures of Methylene Blue and Methyl Orange by Ag/ZnO under UV-irradiation were performed in [22].

Mechanisms of the degradation of three different dyes on La doped ZnO photocatalyst using visible light was presented in [23]. The photocatalytic degradation of Reactive Black 5 dye in distilled and sea water using La/ZnO samples under UV-light irradiation was described in [24]. The photodegradation of the Metasystox, Paracetamol drugs, 2,4,6-trichlorophenol and Methyl Orange dye on La-doped ZnO powders were reported [25-28].

The aim of the present paper is to study comparatively the photocatalytic properties of non-doped and Ag- or La-doped-ZnO photocatalysts obtained by impregnation method for degradation of aqueous solution of Reactive Black 5 dye as model contaminant.

EXPERIMENTAL

The activated ZnO powder was prepared by procedure presented in Bulgarian Patent № 28915/1980 by Shishkov et al. (Cl. Index C 01 G 9/02) [29]. The commercial ZnO was dissolved in nitric acid and after that simultaneous treatment by adding NH₄OH and bubbling CO₂. The obtained precipitate Zn(OH)CO₃ was filtered, washed, dried at 110 °C and thermally treated at 400 °C for 4 h. ZnO powder was impregnated with definite amounts of the aqueous solutions of the AgNO₃ and La(NO₃)₃ (prepared by dissolving of La₂O₃ in nitric

* To whom all correspondence should be sent:

E-mail: kmilenova@ic.bas.bg

acid). The concentrations of Ag and La metal dopants were so preset to give 1.5 wt% metal content with respect to Zn amount. The doped ZnO samples were calcined at 500 °C for 2 h in air atmosphere [30-32].

The powder X-ray diffraction analysis, scanning electron microscopy (SEM) and single point Brunauer-Emmet-Teller (BET) method were used to study the phase composition, morphology and specific surface area of the catalysts. The PXRD patterns were registered on a TUR M62 apparatus with PC control and data acquisition, using HZG-4 goniometer and CoK α radiation. The Scherrer's formula was used to calculate the crystallites size. The morphology of the ZnO photocatalysts surface were investigated by scanning electron microscope (SEM) JEOL, model JEM-200CX, scanning adaptor EM-ASID3D. The specific surface area of the samples was measured in a conventional volumetric apparatus Micromeritics FlowSorb II 2300 (USA) applying single point BET method and using nitrogen adsorption from a mixture 30% N₂+70% He at the boiling temperature of liquid nitrogen (77.4 K). Before determining the specific surface area the materials were degassed at 423 K for 30 min to liberate the entire surface from adsorbed impurities until the residual pressure became lower than 1.333×10^{-2} Pa. The nitrogen (N₂) monolayer formed was used to evaluate the specific surface area (A_{BET}) using the BET equation, whereupon He was the carrier-gas [30-32].

The photocatalytic degradation of Reactive Black 5 (RB5) dye as contaminant in aqueous solution under UV-A polychromatic illumination (18 W) was tested. The change of absorbance during the photocatalytic tests was monitored by UV-Vis absorbance spectrophotometer CamSpec M501 in the wavelength range from 200 to 800 nm, observing especially the wavelength maximum of absorbance at $\lambda_{\text{max}} = 599$ nm for RB5. The initial concentration of RB5 dye was 20 ppm. The studied systems were left in the dark for about 30 min before switching on the UV irradiation in order to reach adsorption-desorption equilibrium state. A semi-batch slurry photocatalytic reactor was used continuously feeding air flow creating large excess of O₂ compared to stoichiometry. The measurements were carried out by taking aliquot samples of the suspension out of the reaction vessel after regular time intervals. The powder was then separated from the aliquot solution by centrifugation before the UV-Vis spectrophotometrical measurements. After that, the aliquot solution, together with the photocatalyst

powder, were returned back quantitatively into the reaction vessel, which ensured the operation under constant volume and constant catalyst amount [30-32].

RESULTS AND DISCUSSION

On the Figure 1 the Powder X-ray diffraction patterns of the undoped and doped ZnO materials are displayed. The presence of ZnO wurtzite phase (PDF-36-1451) was registered in the spectra of the investigated samples. The low content of La and Ag is possible reason explaining the absence of their peaks on the X-ray diffractograms. The determined crystallites size of the studied samples is varying within the range 50÷57 nm (Figure 2). The results established smaller crystallites size of Ag and La doped ZnO (50 and 54 nm) compared to the non-doped ZnO sample (57 nm). The SEM images of the Ag and La doped ZnO materials are presented in Figure 3. The smaller size of the particles is observed for Ag doped ZnO than that in the case of La dopant. The aggregates consisting of nanosized particles with irregular shape can be seen on the Figure 3. The Ag-ZnO (32 m²/g) and La-ZnO (30 m²/g) doped photocatalyst samples possess somewhat higher specific surface areas compared to that of the pure ZnO (19 m²/g) [30-32].

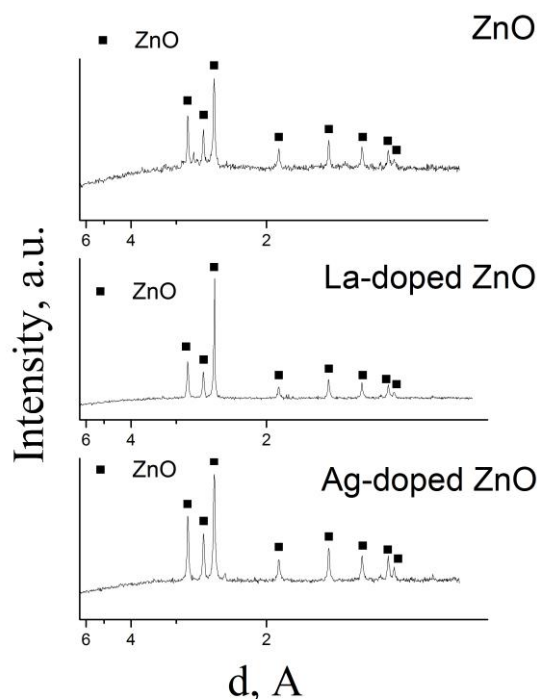


Fig. 1. PXRD patterns of studied non-doped and doped ZnO samples.

The adsorption capacities of non-doped and doped ZnO samples after 30 minutes dark period

(adsorption discoloration) were calculated by the equation:

$$Q = \frac{(C_0 - C) \cdot V}{m} \quad (1)$$

where C_0 and C are the initial and after 30 minutes in the dark concentrations of the dye, V is the volume of the solution and m is the weight of the catalyst.

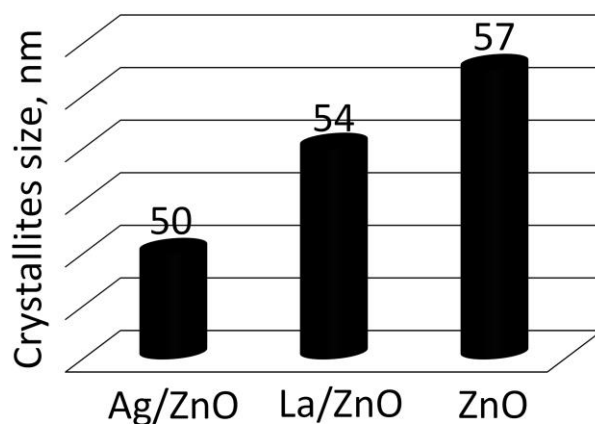


Fig. 2. Crystallites size of investigated non-doped and doped ZnO materials.

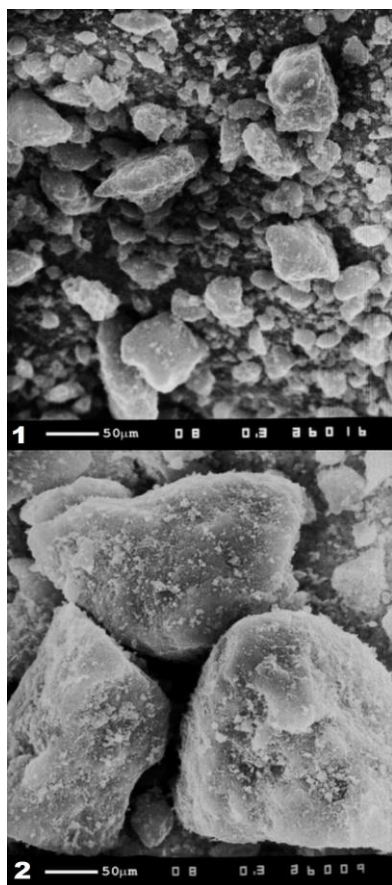


Fig. 3. SEM images of 1 - Ag doped ZnO and 2 - La doped ZnO photocatalysts

The adsorption capacities of the investigated samples decrease in the following order: ZnO (0.028 mg/g) > La-ZnO (0.025 mg/g) > Ag-ZnO (0.018 mg/g).

Figure 4 presents concentration changes of RB5 dye related to the surface area of the photocatalyst based on the changes in the intensity of the

maximal absorbance at 599 nm with time under UV irradiation. Photocatalytic degradation degree of RB5 dye on the studied samples are different for doped and undoped zinc oxide photocatalysts. We observed lower activity for ZnO, while doping with

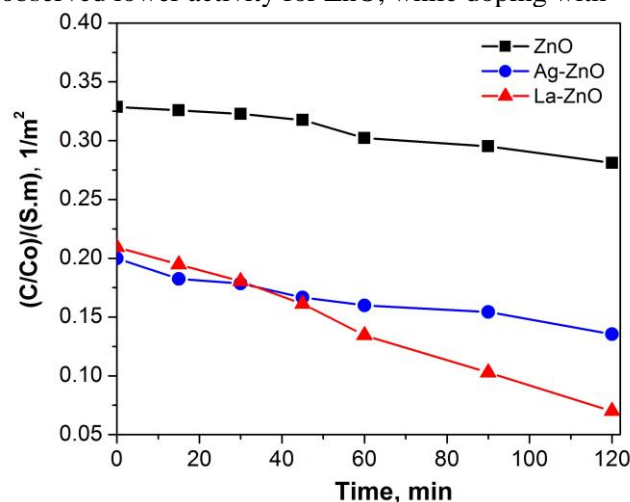


Fig. 4. Concentration changes of RB5 dye related to the surface area of the photocatalyst based on changes in the intensity of the maximal absorbance at 599 nm corresponding to the peak of the diazo bond (-N=N-) for RB5 respectively, with the course of time under UV-A irradiation

Ag and La improved it especially in the case of La-ZnO sample. Figure 5 illustrates the reaction course of dye degradation of investigated catalysts with the time of illumination. The results for degradation conversion degrees are in correlation with those of Figure 4 as they followed the order of activities: ZnO (20%) < Ag-ZnO (35%) < La-ZnO (69%). The degradation apparent rate constants (pseudo first order kinetics) have been calculated using logarithmic linear dependence of the concentrations

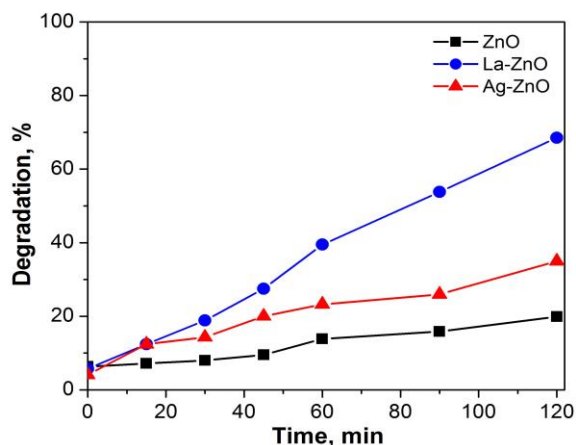


Fig. 5. Degradation of Reactive Black 5 dye calculated as $[(C_0-C)/C_0] \times 100, \%$ with the course of time under UV-A illumination at 599 nm absorbance maximum, attributed to the peak of the diazo bond ($-N=N-$) for RB5 using non-doped and Ag and La doped ZnO photocatalysts.

ratio on the time: $-\ln(C/C_0) = k.t.$ and they are represented in Figure 6. The highest photocatalytic activity is demonstrated by La doped ZnO photocatalyst. In comparison with our previous work on La-ZnO photocatalyst this new sample possesses higher value of the rate constant than those of Co, Mn, Ni or Cu doped ZnO samples [32].

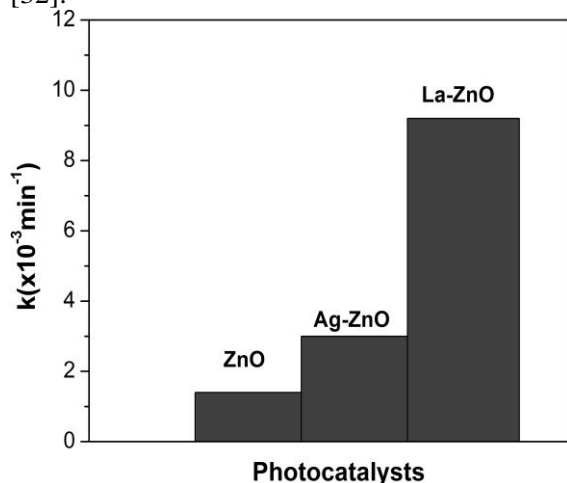
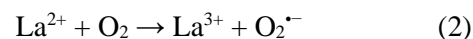


Fig. 6. Apparent rate constants of non-doped and Ag and La doped ZnO photocatalysts.

The enhanced photocatalytic activity in oxidative photodegradation of organic compounds is probably due to the decrease in rate of recombination of the photogenerated electron-holes, synergistic effect between dopant and ZnO [10], production of a large number of oxygen vacancies on doped ZnO, which strongly adsorb OH^- [27]. Among the lanthanides doped ZnO catalysts, La/ZnO shows the best photocatalytic activity because of: higher dark adsorption capacity, electron accepting ability, more OH radical production capability [28].

The doped photocatalysts have higher specific surface area than the non-doped ZnO. The higher photocatalytic efficiency of La-ZnO samples, compared to that of Ag/ZnO, can be explained in terms of differences in dark adsorption capacity and higher degree of crystallinity.

The superiority of the La/ZnO photocatalytic material is probably due to the interplay of the $\text{La}^{3+} \leftrightarrow \text{La}^{2+}$ ion pair representing an oxidation/reduction catalytic cycle, whereupon the reduction of La^{3+} ions into La^{2+} ions is caused by the photoexcited electrons, while the oxidation of La^{2+} into La^{3+} is caused by the oxygen molecules in large stoichiometric excess in comparison to the pollutant concentration in a semi-batch reactor feeding continuously air to the photoreactor (equation 2). This interplay of an ion couple is missing in the case of Ag/ZnO sample.



Similar supposition has been put forward by Okte [28]. The produced superoxide anion-radical ($\text{O}_2^{\cdot-}$) is responsible for the generation of highly reactive $\cdot\text{OH}$ radicals, due to their electrophilic nature.

In the meantime, photogenerated holes may react with H_2O molecules and produce $\cdot\text{OH}$ radicals. Thus, loading of lanthanum ions on the surface of ZnO matrix can suppress the recombination of photoinduced charge carriers either with only electron capture ability or with steps forward to produce $\cdot\text{OH}$ radicals.

CONCLUSIONS

The present study on the photocatalytic behavior of Ag and La doped ZnO materials in the oxidative degradation of aqueous solutions of RB5 dye under UV light, shows that the doping affects the photocatalytic activity, the crystallite size and the specific surface area of ZnO material. The Ag and La doping of ZnO lead to increase in the photocatalytic activity and specific surface area and decrease in the crystallite size, comparing with those characteristics of the non-doped ZnO material. Lanthanum doped ZnO photocatalyst exhibited higher efficiency in the oxidative degradation of RB5 dye than Ag doped ZnO samples due to the interplay between La^{2+} and La^{3+} ions, which effect is missing in the case of Ag dopant.

Acknowledgements: The authors gratefully acknowledge financial support by National Science Fund, Ministry of Education and Sciences of Bulgaria (Contract DFNI- T-02 16).

REFERENCES

1. K. M. Lee, C. W. Lai, K. S. Ngai, J. C. Juan, *Water Res.*, **88**, 428 (2016).
2. I. Daou, O. Zegaoui, A. Elghazouani, *C. R. Chimie*, **20**, 47 (2017).
3. N. Tripathy, R. Ahmad, H. Kuk, Y.-B. Hahn, G. Khang, *Ceram. Int.*, **42**, 9519 (2016).
4. S. Akir, A. Barras, Y. Coffinier, M. Bououdina, R. Boukherroub, A. D. Omrani, *Ceram. Int.*, **42**, 10259 (2016).
5. Y.-C. Weng, K.-T. Hsiao, *Int. J. Hydrogen Energ.*, **40**, 3238 (2015).
6. S. Mohammadzadeh, M. E. Olya, A. M. Arabi, A. Shariati, M.R. Khosravi Nikou, *J. Environ. Sci.*, **35**, 194 (2015).
7. Q. Huang, Q. Zhang, S. Yuan, Y. Zhang, M. Zhang, *Appl. Surf. Sci.*, **353**, 949 (2015).
8. J. Kaur, K. Gupta, V. Kumar, S. Bansal, S. Singhal, *Ceram. Int.*, **42**, 2378 (2016).
9. K. Saoud, R. Alsoubaihi, N. Bensalah, T. Bora, M. Bertino, J. Dutta, *Mater. Res. Bull.*, **63**, 134 (2015).
10. X. Hou, *Mater. Lett.*, **139**, 201 (2015).
11. H. Liu, Y. Hu, Z. Zhang, X. Liu, H. Jia, B. Xu, *Appl. Surf. Sci.*, **355**, 644 (2015).
12. H. Zhai, L. Wang, D. Sun, D. Han, B. Qi, X. Li, L. Chang, J. Yang, *J. Phys. Chem. Solid.*, **78**, 35 (2015).
13. R. Aladpoosh, M. Montazer, *Carbohydr. Polymer.*, **141**, 116 (2016).
14. S. S. Patil, M. G. Mali, M. S. Tamboli, D. R. Patil, M. V. Kulkarni, H. Yoon, H. Kim, S. S. Al-Deyab, S. S. Yoon, S. S. Kolekar, B. B. Kale, *Catal. Today*, **260**, 126 (2016).
15. H. Bouzid, M. Faisal, F.A. Harraz, S. A. Al-Sayari, A. A. Ismail, *Catal. Today*, **252**, 20 (2015).
16. D. Zhang, X. Pu, H. Li, Y. M. Yu, J. J. Shim, P. Cai, S. I. Kim, H. J. Seo, *Mater. Res. Bull.*, **61**, 321 (2015).
17. Q. Deng, H. Tang, G. Liu, X. Song, G. Xu, Q. Li, D. H. L. Ng, G. Wang, *Appl. Surf. Sci.*, **331**, 50 (2015).
18. R. Kumar, D. Rana, A. Umar, P. Sharma, S. Chauhan, M. S. Chauhan, *Talanta*, **137**, 204 (2015).
19. M. Khademalrasool, M. Farbod, A. Irajizad, *J. Alloy Comp.*, **664**, 707 (2016).
20. J. Wang, Y. Xia, Y. Dong, R. Chen, L. Xiang, S. Komarneni, *Appl. Catal. B Environ.*, **192**, 8 (2016).
21. Y. I. Choi, H. J. Jung, W. G. Shin, Y. Sohn, *Appl. Surf. Sci.*, **356**, 615 (2015).
22. M. A. Chamjangali, G. Bagherian, A. Javid, S. Boroumand, N. Farzaneh, *Spectrochim. Acta Mo. Biomol. Spectros.*, **150**, 230 (2015).
23. W. Raza, M. M. Haque, M. Muneer, *Appl. Surf. Sci.*, **322**, 215 (2014).
24. N. Kaneva, A. Bojinova, K. Papazova, D. Dimitrov, *Catal. Today*, **252**, 113 (2015).
25. P. V. Korake, R. S. Dhabbe, A. N. Kadam, Y. B. Gaikwad, K. M. Garadkar, *J. Photochem. Photobiol. B: Biol.*, **130**, 11 (2014).
26. M. Shakir, M. Faraz, M. Asif Sherwani, S. I. Al-Resayes, *J. Lumin.*, **176**, 159 (2016).
27. M. Samadi, M. Zirak, A. Naseri, E. Khorashadizade, A. Z. Moshfegh, *Thin Solid Films*, **605**, 2 (2016).
28. A. Neren Ökte, *Appl. Catal. A: Gen.*, **475**, 27 (2014).
29. D. Shishkov, C. Velinova, N. Kassabova, C. Canov, D. Ivanov, D. Klissurski, V. Iordanova, I. Uzunov, Method of preparation of activated zinc oxide. Bulgarian Patent 28915/1980 (Classification Index C 01G 9/02) (in Bulgarian) (1980).
30. K. Milenova, A. Eliyas, V. Blaskov, I. Stambolova, S. Rakovsky, *Journal of International Scientific Publications: Materials, Methods & Technologies*, **8**, 259 (2014).
31. K. Milenova, A. Eliyas, V. Blaskov, I. Stambolova, B. Kunev, S. Rakovsky, *Journal of International Scientific Publications: Materials, Methods & Technologies*, **8**, 265 (2014).
32. K. Milenova, I. Avramova, A. Eliyas, V. Blaskov, I. Stambolova, N. Kassabova, *Environ. Sci. Pollut. Res.*, **21**, 12249 (2014).

ЕФЕКТИВНОСТ НА ZnO ФОТОКАТАЛИЗАТОРИ ДОТИРАНИ С Ag И La

К. И. Миленова^{1*}, К. Л. Захариева¹, И. Д. Стамболова², В. Н. Блъсков², А. Е. Елияс¹

¹Институт по катализ, Българска академия на науките, ул. „Акад. Г. Бончев“, бл. 11, 1113 София, България

²Институт по обща и неорганична химия, Българска академия на науките, ул. „Акад. Г. Бончев“, бл. 11, 1113 София, България

Постъпила на 27 юни, 2016 г. коригирана на 11 ноември, 2016 г.

(Резюме)

Фотокаталитичната ефективност на Ag и La дотирани ZnO материали, получени чрез импрегниране и последваща термична обработка, беше изследвана и сравнена в реакцията на окислително разграждане на Реактивно Черно 5 багрило (PЧ5) като моделен замърсител във водни разтвори под действието на УВ светлина. Структурата, фазовия състав, морфологията и специфичната повърхност на недотирани и дотирани ZnO фотокатализатори бяха изследвани чрез рентгенова дифракция, сканираща електронна микроскопия и БЕТ метод. Резултатите установиха, че най-висока степен на разграждане на PЧ5 багрило (69%) след 120 минути осветяване беше постигната използвайки La дотиран ZnO фотокатализатор в сравнение с другите проби - Ag дотиран ZnO (35%) и недотиран ZnO (20%). Скоростните константи на разграждане на PЧ5 багрилото намаляват в следния ред: La-ZnO ($9.2 \times 10^{-3} \text{ min}^{-1}$) > Ag-ZnO ($3 \times 10^{-3} \text{ min}^{-1}$) > ZnO ($1.4 \times 10^{-3} \text{ min}^{-1}$) дължащо се на обменно взаимодействие на La²⁺ и La³⁺ двойка йони.